Analysis of PAHs and PCBs in Fogwater at Urban, Suburban, and Rural Sites in North East France

Dani Khoury , Maurice Millet * , Yasmine Jabali , Olivier Delhomme

Posted Date: 31 January 2024

doi: 10.20944/preprints202401.2191.v1

Keywords: Strasbourg metropolitan; persistent organic pollutants; diagnostic ratio

Article

Analysis of PAHs and PCBs in Fogwater at Urban, Suburban, and Rural Sites in North East France

Dani Khoury [1,2], Maurice Millet [1,*], Yasmine Jabali [2] and Olivier Delhomme [1,3]

[1] Institute of Chemistry and Processes for Energy, Environment and Health ICPEES, UMR 7515 Group of Physical Chemistry of the Atmosphere, University of Strasbourg, Strasbourg, France; dani.khoury@u-bordeaux.fr

[2] Environmental Engineering Laboratory (EEL), Faculty of Engineering, University of Balamand, P.O. Box 100, Kelhat-El Koura, Tripoli, Lebnaon; yasmine.jabaly@balamand.edu.lb

[3] UFR Sciences Fondamontales et Appliquées, University of Lorraine, Rue du General Deslestraint, 57070 Metz, France; olivier.delhomme@univ-lorraine.fr

* Correspondence: mmillet@unistra.fr; Tel.: +33-(0)368-852-866

Abstract: Polycyclic aromatic hydrocarbons (PAHs) and polychlorinated biphenyls (PCBs) exist in the atmosphere in the vapor and particulate phases, as well as in the solubilized form in fog/rain/cloud waters. They are abundant pollutants and are known for their acute and chronic toxicity. In the current paper, fogwater samples are collected during 42 events between 2015 and 2021 at four sites (Strasbourg, Geispolsheim, Erstein, Cronenbourg) in the Alsace region with different topological characteristics. PAHs and PCBs are extracted using the liquid-liquid extraction (LLE) supported on a solid cartridge (XTR Chromabond), and then analyzed by gas-chromatography tandem mass spectrometry (GC-MS/MS). Total PAHs and PCBs concentration in fog samples varied between 0.58 and 6.7 μg L^{-1} (average of 2.70 μg L^{-1}), and 0.14 and 15.5 μg L^{-1} (average of 2.75 μg L^{-1}). Low molecular weight (LMW) predominant and highly detectable over high molecular weight PAHs by at least 1.6 times, while pentachloro-biphenyls are the dominant PCB congener accounting for at least 50% of the total fraction. PAHs and PCBs concentrations have increased over sampling years at all sites, except a slight decrease in PCBs level at Geispolsheim. Diagnostic ratio analysis suggested that diesel and fossil fuel combustion are the dominant contributors to PAHs in Alsace.

Keywords: Strasbourg metropolitan; persistent organic pollutants; diagnostic ratio

1. Introduction

Fogwater is a meteorological phenomenon that is composed of water droplets condensed in the air [1,2]. It has the ability to scavenge inorganic compounds as well as organic compounds through various mechanisms including nucleation scavenging, coagulation, Brownian diffusion, and uptake of precursor gases with subsequent transformation [3–6]. The main environmental benefit toward fogwater refers to its high ability to decrease the ambient pollutant concentration through continuous nucleation scavenging followed by wet deposition [7,8]. However, it may promote the formation of new particles via aqueous- phase reactions [9–11]. Persistent organic pollutants (POPs), such as PAHs and PCBs, are amongst the organic species that can be scavenged by fogwater [12,13]. POPs are highly stable and long-lasting that may persist in the atmosphere for extended period of time compared to other toxics [14]. They are characterized by their high potential to degradation and their ability to be transported through different environmental (air, water, and soil) and biological matrices. They can enter the environment through unintentional and intentional routes resulting from diesel, fossil fuel combustion, agricultural activities, etc. [15]. POPs are linked with adverse impacts on human and the environment. Long-term exposure to some POPs has been associated to developmental abnormalities, endocrine disruption, and increased cancer risks [14,16]. Numerous studies have been

 doi:10.20944/preprints202401.2191.v1

performed on PAHs and PCBs occurrence and distribution in the aquatic system (river, lakes, etc.) [17–19], soil [20–22], and air [23–26], of which very few ones were performed in fogwater [2,27–29]. Although there are many PAHs, most analyses and regulations focus on a limited number of PAHs, which are recognized by the Environmental Protection Agency (EPA) as harmful components (16 PAHs) [30]. Once released into the atmosphere, they can be found in the gas or particulate phase. PAHs with 2 to 3 rings (LMW) tend to be more concentrated in the gas phase, whereas those with 4 to 6 rings (HMW) are found in the particulate phase [31]. PCBs have been widely used since long time in a wide variety of industrial applications such as electrical transformers and capacitors, hydraulic fluids, lubricants, paints, heat transfer fluids, etc. PCBs are classified based on the degree of chlorination (low and high chlorinated PCBs). The degree of their toxicity increases with their number of chlorine atoms [32]. Therefore, it is crucial to investigate the occurrence of both PAHs and PCBs in fog events.

Alsace region is known for its radiation fog that is formed during stable weather conditions (calm wind) at nights. Strasbourg is known for its high population density which contributed to harmful contamination in the city itself, and its surrounding regions by releasing various pollutants. To better understand the environmental and health impacts of PAHs and PCBs, 38 fog events are sampled at four different sites which are Strasbourg (urban), Geispolsheim (suburban), Erstein (rural), and Cronenbourg (suburban) during 2015, 2016, and 2018. Additionally, only one fog event is sampled during 2017 at Geispolsheim, while three were sampled during 2021 at Cronenbourg due to the absence of fog events at other sites. The analysis of fogwater at Strasbourg started in early 1990's and lasted until the end of 1999 [33,34]. Since then, there are no fog studies that have been conducted in Alsace. The current paper aimed to use LLE on a solid support (XTR Chromabond) along with GC-MS/MS to assess PAHs and PCBs in fog events. The global aim of this study is to have a primary database regarding fogwater contamination in Alsace to perform statistical analyses at the end which involve inorganics, organics, and microphysics to study the factors that are responsible for spatio-temporal variation. The specific objectives of this research are (1) monitoring PAHs and PCBs in fogwater at Strasbourg metropolitan (Alsace) (2) checking the evolution of fogwater over the sampling years (3) identifying the sources of PCBs and PAHs in Alsace.

2. Materials and Methods

2.1. Study Sites

Fogwater samples assessed in the current study are sampled from north-eastern France between October and December between 2015 and 2018 and in 2021. The sites are chosen based on their topological variability. Strasbourg (48.58461°, 7.75071°), in the middle, is a typical urban site surrounded by huge residential areas (284.677 inhabitants) and traffic. It is in close proximity (3 Km away) with the biggest industrial zone in the region, known as the "Port du Rhin". Two suburban sites, Cronenbourg (48.59449°, 7.71621°) and Geispolsheim (48.51469°, 7.64373°), located respectively in the north-west and west Strasbourg. Geispolsheim is enclosed by small houses (7,000 inhabitants) and agricultural fields, and far around 1 Km from the A35 highway and 9 Km from Entzeim airport. Cronenbourg is surrounded by bigger residential areas (21,000 inhabitants) and limited industries. Erstein (48.42345°, 7.66326°), is a rural site (11,000 inhabitants) situated south-west Strasbourg characterized by its wider agricultural fields. The sampling sites are shown in Figure 1.

 doi:10.20944/preprints202401.2191.v1

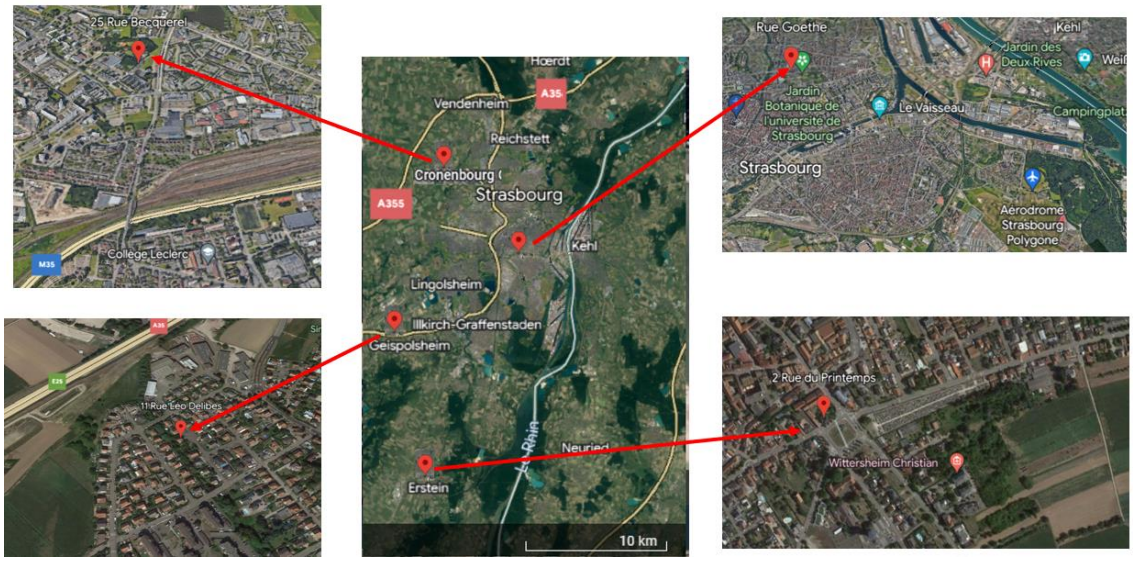

Figure 1. Study site showing the location of the four sampling locations.

2.1. Sampling Campaign

The sampling campaign was mainly performed between 2015 and 2018 during October, November, and December (foggy periods in Alsace) to get a total of 39 samples. Additionally, 3 samples are gathered only at Cronenbourg during 2021 due to the absence of foggy days. At each sampling site, fog samples are collected using a Caltech Active Strand Cloudwater collector (CASCC2) described in detail elsewhere [35]. Field blanks are taken continuously after cleaning the collector to assure the absence of any contamination during the sampling period. More details for the collection procedure are found in [12,36]. Table S1.1 in the Supplementary Material show the date and time of the different samples at all sites.

2.2. Analytical Procedure of Fogwater Samples

Samples are analyzed for their potential contamination in 22 PCBs and 16 PAHs analyzed by GC-MS/MS. The lists of the analyzed compounds are listed in the Supplementary Material. The analytical procedure used for the analysis is based on the work of Khoury et al. for the residual analysis of organic compounds in fogwater [12].

2.1.1. Samples Treatment

Fog samples are filtered on-site (glass microfiber, 0.47 µm porosity), transported refrigerated to the ICPEES laboratory, and separated into many aliquots. The first aliquot is used for pH, conductivity, and dissolved organic carbon (DOC, total organic carbon analyzer) measurements, another aliquot to quantify cations and anions (ion chromatography), a third aliquot to measure trace metals (inductively coupled plasma mass spectrometry), another aliquot to analyze different organic families. Fog samples are maintained in clean glass bottles and frozen at -18°C where they are stored until further analysis. In the current paper, we present only the results of the determination of PAHs and PCBs for the different fog events in the studied areas. The full handling protocol is found in Khoury et al. [12,36].

2.1.2. Extraction Procedure

The extraction protocol is fully described in Khoury et al. [12]. Liquid-liquid extraction (LLE) on a solid cartridge (XLB Chromabond) is used for extraction of PAHs and PCBs in fog samples. A volume of 50 mL of fog sample is loaded into the column and the elution is performed successively with 40 mL of dichloromethane (DCM) and 40 mL of ethyl acetate (EtAc). The extract is gently evaporated under fume hood to 1 mL. The chromatographic analysis is performed by GC-MS/MS

 doi:10.20944/preprints202401.2191.v1

following the addition of the appropriate mixture of the internal standard (IS). Laboratory blanks (solvent) are also performed continuously between sample injections to remove any trace/contamination in the instrument. The validation parameters for PAHs and PCBs along with the internal standard mixture are shown from Tables S1.2–S1.6 in the Supplementary Material.

2.1.3. Chromatographic Analysis

The analytical parameters for the analysis of PAHs and PCBs are summarized by Table 1. The identification of the different species is based on the Multiple reaction monitoring (MRM) mode. The accurate detection of each compound detected is done by checking and comparing the observed retention times, parent ions, and fragmented (daughter) ions with those obtained for standard solutions. The results are treated using linear calibration curves which are performed on Xcalibur.

Table 1. Analytical conditions for the analysis of PAHs and PCBs with GC-MS/MS.

Chromatographic conditions	
Device	GC-MS/MS (Trace™, ITQ™ 700)
Separation column	XLB (50% phenyl/ 50% methylsiloxane) (30 m length, 0.25 mm diameter, 0.25 µm film thickness)
Injection parameters	
DCM Rinsing	2 Rinsing with 1µL (pre-run and post-run)
Injection volume	1 µL
Injection type	Splitless mode
Injector temperature	250°C
Purge	50 mL.min^{-1} after t = 2 min
Gas saver	15 mL.min^{-1} after t = 5 min
Chromatographic parameters	
Carrier gas	Helium (purity >99.99%)
Carrier gas flow	Constant at 1 mL.min^{-1}
Pressure	≈10.253 psi (à t=0 et T= 90°C)
Oven temperature programming	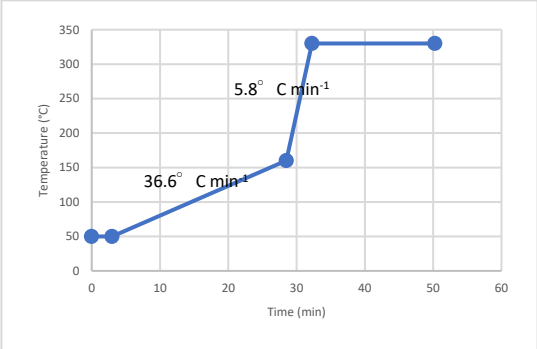
Mass spectrometer parameters	
Transfer line temperature	300 °C
Electron energy	70 eV
Source temperature	210 °C
Acquisition mode	MRM

 doi:10.20944/preprints202401.2191.v1

3. Results and Discussion

3.1. PAHs Analysis in Fogwater

In this investigation, PAHs are divided into LMW and HMW PAHs, according to the number of the benzene rings. LMW PAHs include Naphtalene (NaP), Acenaphtene (Ace), Fluorene (Flu), phenanthrene (Phe) and anthracene (Ant). HMW PAHs include Fluoranthene (Flo), Pyrene (Pyr), Chrysene (Chry), Benzo(a)anthracene (BaA), Benzo(b)fluoranthene (BbF), Benzo(k)fluoranthene (BkF), Benzo(e)pyrene (BeP), Benzo(a)pyrene (BaP), Dibenzo(a,h)anthracene (DBhA), Indenol(1,2,3)pyrene (IndP), and Benzo(g,h,i)perylene (BghiP). LMW PAHs (2–3 rings) tend to be more concentrated in the gas phase and could be scavenged by fog water due to their higher solubility, while those with a higher molecular weight (4–6 rings) are often associated with particulates due to their higher hydrophobicity. The common PAHs detected in most analyzed fog samples mostly belong to the LMW PAHs like NaP, Flu, Phe and Ant. HMW PAHs are rarely found in fog water. For instance, BaA, Chry, BbF, BkF, BeP, BaP, and DBhA are monitored yearly once or twice per site. BaP is regarded as a marker of total carcinogenic PAH compound, fortunately it is not detected too much in this investigation. The detection frequency (DF) for LMW PAHs is higher than 96%, whereas that of HMW PAHs varies from 0 to 96%. The DF of Flo, Pyr, IndP, and BghiP is respectively 96%, 91%, 77%, and 56%, whereas the rest is detected with less than 30%. Over the sampling years, the concentrations of LMW PAHs are several times higher than those of HMW PAHs at all sampling sites. The ratios of HMW/LMW PAHs are all lower than 1 (varying from 0.1 to 0.5) suggesting that pyrogenic activities predominant over petrogenic activities. Those results are in accordance with previous fog studies [13,27].

The mean concentrations of LMW and HMW PAHs at the four sites during the sampling years are summarized in Figure 2 (see Table S2.1 in the Supplementary Material). LMW PAHs account between 67 and 85% (average of 78%), 61 and 89% (average of 77%), 82 and 95% (average of 88%), and 81 and 88% (average of 83%) of the total PAH concentrations respectively at Geispolsheim, Erstein, Strasbourg, and Cronenbourg. Their mean concentrations respectively vary from 0.17 to 1.15 μg L^{-1}, 0.05 to 0.51 μg L^{-1}, 0.31 to 0.87 μg L^{-1}, and 0.03 to 1.58 μg L^{-1}. The main source of PAHs is mainly due to the consumption of large amounts of fuel combustion that are conducted during wintertime (fog period) in the Alsace region (October, November, and December), which most probably lead high PAH emission which appeared in the analysis of fogwater. The total PAH concentrations vary according to the sampling site and year. The highest total mean concentration is obtained at Erstein (2.99 ± 0.25 μg L^{-1}) followed by Geispolsheim (2.91 ± 0.34 μg L^{-1}), Cronenbourg (2.77 ± 1.70 μg L^{-1}) and Strasbourg (2.40 ± 0.93 μg L^{-1}). A slight increase in the total mean concentration is observed yearly at all sampling sites. For instance, the total mean concentrations have increased at Geispolsheim from 2.53 to 3.34 μg L^{-1} (+33%) between 2015 and 2018, Erstein from 2.71 to 3.21 μg L^{-1} (+18%) between 2015 and 2018, Strasbourg from 1.75 to 3.06 μg L^{-1} (+74%) between 2016 and 2018, and Cronenbourg from 1.57 to 3.97 μg L^{-1} (+153%) between 2018 and 2021. The high increase at Cronenbourg might be due to the post-covid pandemic period. France experienced the total confinement period during Covid-19 in which people stayed at home, suggesting that PAH concentrations are closely associated with some additional anthropogenic activities such as more wood and coal burning for domestic heating.

Preprints.org (www.preprints.org) | NOT PEER-REVIEWED | Posted: 31 January 2024 doi:10.20944/preprints202401.2191.v1

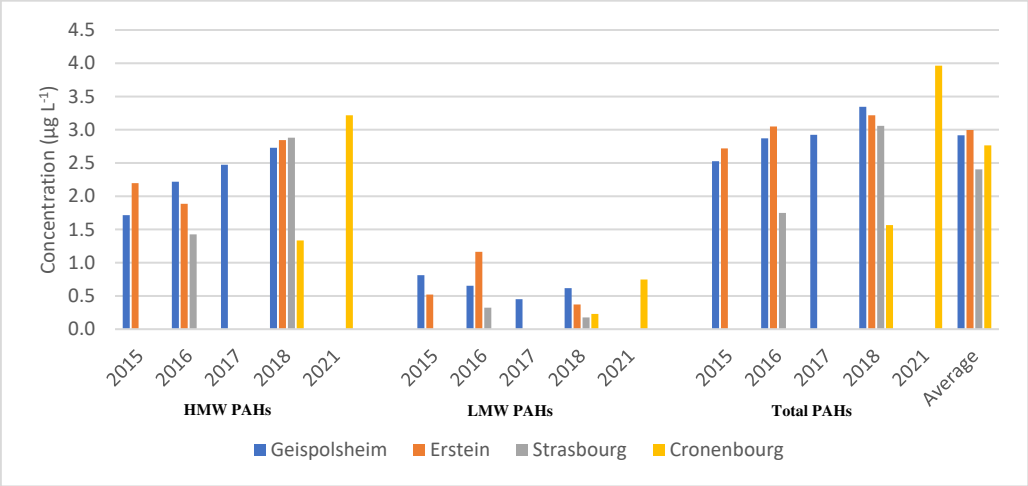

Figure 2. Spatio-temporal variation of PAHs at the different sites and years.

The % contributions of PAHs, shown in Figure 3, correspond to the sum of the average concentration for each PAH compound at each site to the total PAH concentrations at that site during all years. Nap, Phe, and Ant have the highest contributions in all analyzed fog water samples at all locations. Ant has the highest contribution which varies between 25.3 and 38.9 % (average of 35.2%), followed by Phen which varies between 19.1 and 30.1% (average of 24.5%), and Nap which varies between 10.5 and 20.2 % (average of 14.9%). Their average concentrations are respectively 2.68, 1.79, and 1.21 µg L^{-1}. The % contributions of other PAHs are less than 10%. HMW PAHs have low contributions in fog water samples (as low as 1%), except for Pyr and Flo whose average % contributions are respectively 6.9 and 4.9 %, with average concentrations respectively of 0.54 and 0.39 µg L^{-1}.

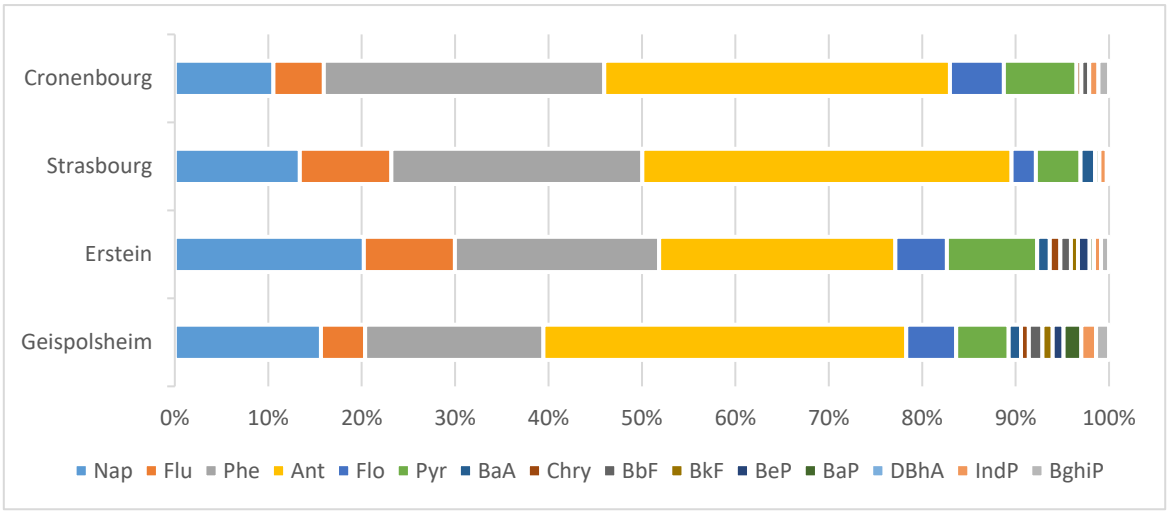

Figure 3. Average contribution of the different PAHs.

PAHs are considered as a single hopper suggesting that all sites might be affected by the emissions released from neighboring industries and power plants. In the current study, source identification of PAHs is conducted by using the diagnostic ratio (DR) method. It is used to differentiate between gasoline and diesel combustion emissions, and between biomass burning processes and different crude oil processing products [37]. Subsequently, DR method is performed through establishing an index based on the ratio of the PAHs having the same molecular weight (MW) [38]. PAHs with molecular weights of 178 and 202 are commonly used to differentiate between combustion and petroleum source. For a PAH with a molecular weight of 178, when the ratio of Ant/(Ant + Phe) is below 0.1, it indicates petroleum origins. In case the ratio is beyond 0.1, it indicates

 doi:10.20944/preprints202401.2191.v1

combustion emissions. For an individual PAH compound with a molecular weight of 202, when the ratio of Flo/(Flo+Pyr) is below 0.4, it indicates petroleum source. When the ratio is between 0.4 and 0.5, it indicates fossil fuel combustion (vehicle and crude oil), whereas the source is suggestive of grass, wood or coal combustion when the ratio is beyond 0.5. Besides, in case the ratio of Flu/(Flu+Pyr) is lower than 0.5, it indicates that PAHs originate from petroleum emissions. Whereas, a ratio is higher than 0.5, then it indicates diesel emissions. Other DRs, which are used in previous studies, cannot be applied in our case, because the DF of HMW PAHs is very low in our samples. The average ratios of Ant/(Ant+Phe), Flu/(Flu+Pyr), and Flo/(Flo+Pyr) at the four sites during the sampling years are shown in Table 2. The results reveal that the ratios of Ant/(Ant+Phe) are all higher 0.1 indicating pyrogenic emissions. For instance, the average ratios at Geispolsheim, Erstein, Strasbourg, and Cronenbourg are respectively 0.61 ± 0.09, 0.51 ± 0.13, 0.54 ± 0.09, and 0.54 ± 0.02. Pyrogenic sources might include the incomplete combustion of organic matters (fossil fuel, coal, wood, and petroleum), forest fires, by-products of industrial processing and vehicle engines powered by gasoline or diesel fuel. In addition, most of the Flu/(Flu+Pyr) ratios are higher than 0.5 suggesting that diesel emission is one of the sources in the region. Diesel emissions are mainly released from the transportation sector (automobile traffic with diesel vehicles and heavy-duty trucks) [39]. For instance, the average ratios at Geispolsheim, Erstein, Strasbourg, and Cronenbourg are respectively 0.56 ± 0.2, 0.6 ± 0.12, 0.68 ± 0.24, and 0.52 ± 0.12. Furthermore, the results show that the average ratios of Flo/(Flo+Pyr) at Erstein, Strasbourg, and Cronenbourg are respectively 0.41 ± 0.07, 0.45 ± 0.07, and 0.42 ± 0.08 which are all between 0.4 and 0.5 suggesting that PAHs also originate from fossil fuel combustion. Geispolsheim is the only site at which most of the average values of Flo/(Flo+Pyr) are higher than 0.5 (0.52 ± 0.07) indicating that PAHs are released from the combustion of grass, wood, and coal. In the Alsace region, more than 87% of PAHs are originated either from domestic heating (based on wood or coal) or transportation sector (diesel and gasoline combustion). These data are in accordance with the results obtained in this work [40].

Table 2. Average diagnostic ratios of PAHs at all sites and years.

	ANT/(ANT+PHE)			
	Geispolsheim	**Erstein**	**Strasbourg**	**Cronenbourg**
2015	0.50±0.2	0.40		
2016	0.56±0.18	0.46±0.15	0.46	
2017	0.72			
2018	0.65±0.1	0.65±0.13	0.60±0.12	0.56±0.28
2021				0.52±0.12
AVERAGE	**0.6±0.09**	**0.51±0.13**	**0.53±0.09**	**0.54±0.02**
	FLU/(FLU+PYR)			
	Geispolsheim	**Erstein**	**Strasbourg**	**Cronenbourg**
2015	0.41±0.18	0.63		
2016	0.73±0.22	0.47±0.28	0.51	
2017	0.36			
2018	0.74±0.10	0.72±0.13	0.86±0.06	0.60±0.02
2021				0.42±0.15
AVERAGE	**0.56±0.2**	**0.60±0.12**	**0.68±0.24**	**0.52±0.12**
	FLO/(FLO+PYR)			

 doi:10.20944/preprints202401.2191.v1

	Geispolsheim	Erstein	Strasbourg	Cronenbourg
2015	0.58±0.1	0.38		
2016	0.52±0.13	0.49±0.21	0.39	
2017	0.42			
2018	0.55±0.12	0.36±0.11	0.5±0.11	0.36±0.18
2021				0.48±0.12
AVERAGE	**0.52±0.07**	**0.41±0.07**	**0.45±0.07**	**0.42±0.08**

3.2. PCBs Analysis in Fogwater

Figure 4 illustrates the total PCB concentrations at the investigated sites during all years (see Table S2.2 in the Supplementary Material). The highest total PCB concentration is obtained at the urban site Strasbourg, followed by Geispolsheim, Cronenbourg, and Erstein. Their average concentrations are respectively 8.99 ± 2.69 µg L^{-1}, 4.24 ± 2.81 µg L^{-1}, 3.59 ± 1.08 µg L^{-1}, and 2.38 ± 1.90 µg L^{-1}. The total PCB concentrations have increased at Strasbourg, Cronenbourg, and Erstein respectively by 53% (between 2016 and 2018), 54% (between 2018 and 2021), and 188% (between 2015 and 2018). However, a slight decrease has occurred at Geispolsheim by 13% (between 2015 and 2018), despite the substantial decrease between 2015 and 2017 (-85%). It seems that secondary emissions are in the long-term more important than primary emissions.

The average concentrations of the different PCB congeners at all sites are illustrated in Figure 5. In the current analysis, PCBs are classified into different PCB congeners: trichlorobiphenyls include PCBs 18, 28, 31; tetrachlorobiphenyls include PCBs 52, 70, 81; pentachlorobiphenyls include PCBs 101, 105, 114, 118, 123, 126; hexachlorobiphenyls include PCBs 138, 149, 153, 156, 157, 169; and heptachlorobiphenyls include PCBs 189. The repartition of the different PCB congeners is similar at all sampling locations. Figure 6 shows that pentachlorobiphenyls are the dominant congener at all sites, accounting alone for 69, 60, 64, and 51% respectively at Geispolsheim, Erstein, Strasbourg, and Cronenbourg. Their mean concentrations are respectively 2.94, 1.37, 5.75 and 1.83 µg L^{-1}. Hexachlorobiphenyls are the second dominant congeners accounting for 17, 25, 17, and 31% of the total PCB fraction respectively at Geispolsheim, Erstein, Strasbourg, and Cronenbourg. Their average concentrations are respectively 0.70, 0.57, 1.55, and 1.08 µg L^{-1}. Tetrachlorobiphenyl congeners come third, and they contribute between 7 and 13% of the total PCB fraction. Then it comes heptachlorobiphenyls whose contributions are less than 10%, followed by trichlorobiphenyls which have the least contributions (between 1 and 4%) and concentrations.

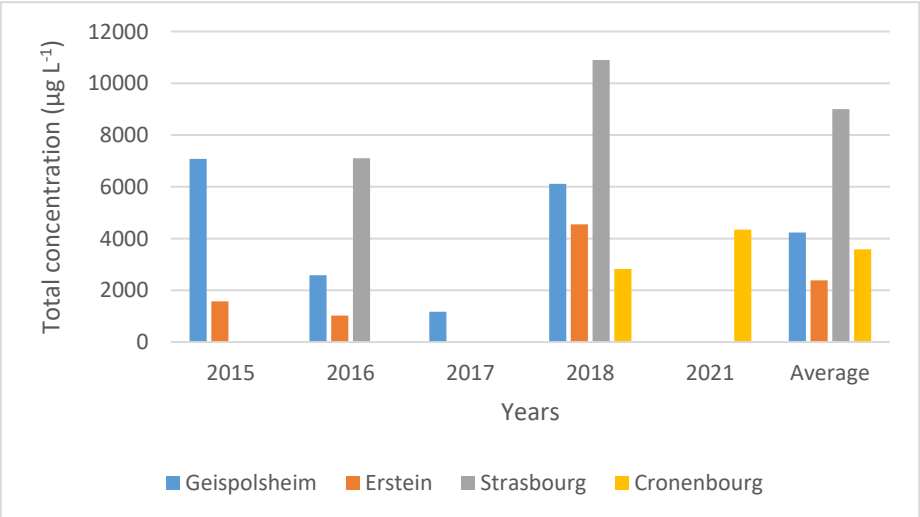

Figure 5. Total PCB concentrations (µg L^{-1}) at all sites and years.

 doi:10.20944/preprints202401.2191.v1

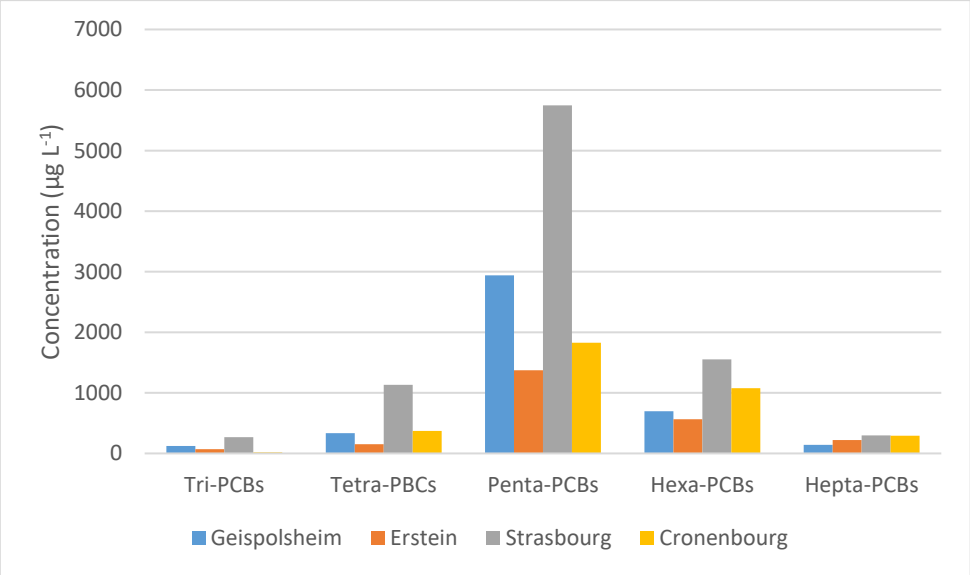

Figure 6. Concentrations (µg L^{-1}) of the different PCB congeners at all sampling sites.

The identification of PCB sources in the environment is more complex than those of PAHs since there are no DRs related to PCB congeners found in literature. Even though their use and production are banned worldwide, they are still be found up to now at important concentrations in the atmosphere. It should be aware that some equipment and materials in some regions are still in use or in stock containing PCBs such as capacitors, vessel paints, double framed glazing windows, etc. [41]. Moreover, in high-density population areas, the high levels of PCBs are not only related to the volatilization process from soil and equipment, but also to the thermal processes that mainly occur during industrial processes, waste incineration, vehicle exhaust, and combustion of organic matters. Basically, five-chlorinated PCBs could be produced as paint additives, while other PCB congeners (>5 chlorine atoms) could be originated from atmospheric deposition released from diesel generators, electric equipment, and vehicles exhaust. Since the distribution of PCB homologs is approximately the same at all sampling sites, therefore their emission sources could be assumed almost the same at the four sampling locations. PCBs 118 and 138 are detected at important concentrations at all sites proving the influence of vehicles and electric equipment as the primary PCB source. Their total mean concentrations are the highest at the urban site (Strasbourg), followed by the two suburban sites (Geispolsheim and Cronenbourg), and the rural site (Erstein). In 2018, PCBs 118 and 138 together have the highest total concentrations (0.98 ± 0.10 µg L^{-1}) at Strasbourg, followed by Geispolsheim (0.22 ± 0.20 µg L^{-1}), Cronenbourg (0.15 ± 0.05 µg L^{-1}), and Erstein (0.06 ± 0.03 µg L^{-1}). The same decreasing order is also observed in 2016 with Strasbourg has the highest total concentrations of PCBs 118 and 138 (0.67 µg L^{-1}), followed by Geispolsheim (0.48 ± 0.61 µg L^{-1}), and Erstein (0.15 ± 0.09 µg L^{-1}). This can be associated to the fact that Strasbourg is the nearest site among others to the industrial port in Kehl "Port du Rhin". Besides, a high load of traffic and vehicles (50,000 vehicles/day) crosses the highway which is only 2 Km far from the sampling point. These two reasons demonstrate the high fraction of PCBs at Strasbourg. The high concentrations of PCBs at Geispolsheim could be also due to its proximity to the highway (A35) through which a huge number of vehicles and trucks passes daily. Other possible sources might be due to the presence of small aluminum and steel factories as well as some energy industries near this region. Moreover, the presence of Entzeim airport may release PCBs due to the incomplete combustion of PCB impurities in fuel, airplane engines, and electric generators. The PCB contamination at Cronenbourg is primarily the result of some traces of PCBs in the soil resulted from one of the biggest breweries "Kronenbourg" in France and Grandest, even if it closed in 2000. This proves the secondary emission sources of PCBs into the air (soil accumulation). At Erstein, PCBs could result from the long-range transport (LRT) of PCBs, in particular, the low chlorine levels congeners (<5 atoms) that are easily degraded in the atmosphere.

 doi:10.20944/preprints202401.2191.v1

Another source could also be attributed to the dependency of rural people on coal and wood for residential heating.

The DF of the analyzed PCBs varies between 27 and 100%. PCBs 105 and 108 are detected in all samples (100%), followed by PCB 189 (98%), PCB 157 (97%), PCB 126 (84%), PCB 70 (72%), and PCB 52 (67%). The least PCBs detected are PCBs 18 and 157 whose DF is 27%. Among the detected PCBs, seven of them are known as the PCBs indicator (∑7PCBs) due to their high abundance in the atmosphere, whereas twelve of them are known as the PCBs dioxin-like (DL) (∑12PCBs) due to their high toxicity and persistency in the atmosphere and their detrimental health effects. The 7 PCBs indicator are 28, 52, 101, 118, 138, 153, and 180, of which six are detected almost in all samples. The 12 PCBs DL are 77, 81, 105, 114, 118, 123, 126, 156, 157, 167, 169, and 189, of which nine are highly detectable in this study. The ∑7PCBs at Strasbourg, Geispolsheim, Cronenbourg, and Erstein are found respectively in the range of 1.25 – 2.38 μg L^{-1} (average of 1.81 μg L^{-1}), 0.26 – 2.09 μg L^{-1} (average of 0.89 μg L^{-1}), 0.24 – 0.46 μg L^{-1} (average of 0.35 μg L^{-1}), and 0.15 – 0.54 μg L^{-1} (average of 0.33 μg L^{-1}). Whereas, the ∑12PCBs vary respectively in the range of 5.14 – 7.28 μg L^{-1} (average of 6.21 μg L^{-1}), 0.82 – 2.29 μg L^{-1} (average of 1.69 μg L^{-1}), 1.34 – 2.39 μg L^{-1} (average of 1.86 μg L^{-1}), and 0.53 – 1.40 μg L^{-1} (average of 0.99 μg L^{-1}). The highest average of both group is obtained at Strasbourg followed by Geispolsheim, Cronenbourg, and Erstein. ∑12PCBs dominates over ∑7PCBs at all sampling sites.

DL-PCBs are classified as non-ortho PCBs with high concern to produce DL-effects, mono-ortho substituted PCBs with a weak ability to produce DL-effects, and multiple-ortho substituted PCBs with no DL-effects [42]. In the following investigation, six PCBs are of major concern which are PCB 77, PCB 81, PCB 105, PCB 114, PCB 118, and PCB 167 due to their similar toxic effect to 2,3,7,8-tetrachlorodibenzo-p-dioxin (2378-TCDD). The decreasing order for $\sum_6$PCBs is: Strasbourg > Geispolsheim > Cronenbourg > Erstein. The total average concentration at Strasbourg is 2.67 μg L^{-1}, Geispolsheim is 0.94 μg L^{-1}, Cronenbourg 0.46 μg L^{-1}, and Erstein is 0.32 μg L^{-1}. The highest $\sum_6$PCBs is obtained at Strasbourg accounting for 30% of the total average PCBs and 43% of $\sum_{12}$PCBs. The least $\sum_6$PCBs is obtained at Erstein accounting for 13% of the total PCBs and 25% of the$\sum_{12}$PCBs. Thus, a high concern might be taking into consideration of these pollutants during pollution management.

In addition, the quantification of potential toxicity is performed by calculating the total toxic equivalent quantity (TEQ). TEQ values are calculated using Equation (1).

$$TEQ = \sum i\ Ci * TEF \quad (1)$$

where Ci is the individual PCB-DL concentration and TEF is the toxic equivalency factors for the six PCBs which are respectively 0.0001, 0.0003, 0.00003 for PCB 77, PCB 81, and PCBs 105, 114, 118 and 167 [43]. The average TEQ is the highest at Strasbourg (0.119) where there are the high-density population and its location near the industrial zone, followed by Geispolsheim (0.039), Cronenbourg (0.022), and Erstein (0.021). Thereby, more attention should be focused on the PCBs congeners with high TEQ contributions.

4. Comparison with Previous Studies

Table 3 summarizes some of previous results showing the mean and/or range of total PAHs concentration. Previous fog studies conducted in China [27,28] and Peninsula [13] prove that fog water is mostly enriched with LMW PAHs rather than HMW PAHs because of the high solubility of LMW PAHs in water. Same dominant compounds are observed at all sites which are Nap, Flu, Phe, Ant, and Flo. The maximum total PAH concentrations observed in Alsace at all sites are lower than other sites, except Erstein which has a higher maximal concentration than that obtained at Shanghai (China). However, the minimum total PAHs concentrations observed are all much higher than those obtained in China and Spain. The mean total PAH concentrations in Alsace are at least about 2.5 times higher than those observed in China. The total concentration of PCBs at Strasbourg varies almost within the same range as that at Zurich (Switzerland), while those observed at other sites are much lower. The total concentrations at the four sites are much higher than those found at Northwestern (Spain).

 doi:10.20944/preprints202401.2191.v1

Table 3. Mean and range of PAH concentrations (ng L^{-1}) in fog samples compared with other sites.

Site	**Mount Taishan (China)**	**Shanghai (China)**	**Northwestern Mountains (Spain)**	**G**	**E**	**STG**	**CR**
Compounds	**[28]**	**[27]**	**[13]**	**This study**	**This study**	**This study**	**This study**
Nap	n.a	376(2-1448)	n.a	534(11-1367)	412(255-1141)	333(158-556)	314(66-554)
Flu	17(5-63)	66(3-520)	18(n.d-134)	112(38-307)	173(22-559)	58(11-88)	180(12-328)
Acy	24(n.d-62)	13(n.d-27)	n.a	n.a	n.a	n.a	n.a
Ace	28(3-53)	30(n.d-114)	n.a	n.a	n.a	n.a	n.a
Phe	80(21-222)	138(3-1043)	n.a	546(145-1920)	750(298-2432)	626(252-1219)	1064(206-1770)
Ant	13(2-25)	172(3-1281)	n.a	1076(152-3181)	851(137-3566)	996(263-2600)	1175(114-1315)
Flo	42(19-95)	34(n.d-178)	n.a	179(23-356)	217(57-496)	226(114-460)	150(103-178)
Pyr	12(1-45)	34(n.d-133)	24(n.d-70)	115(n.d-262)	298(n.d-1259)	97(24-197)	273(63-553)
BaA	13(4-51)	41(n.d-189)	0.1(n.d-1.2)	46(n.d-364.1)	61(n.d-91)	46(n.d-57)	n.d
Chry	9(3-35)	19(n.d-86)	1(n.d-15)	27(n.d-72)	52(n.d-73)	n.d	57(n.d-67)
BeP	9(n.d - 47)	2(n.d-9)	n.a	68(n.d-79)	57(n.d-80)	n.d	n.d
BbF	23(1-102)	4(n.d-22)	0.9(n.d-10)	51(n.d-69)	52(n.d-86)	n.d	46(n.d-56)
BkF	6(n.d - 38)	6(n.d-17)	0.6(n.d-2.1)	67 (n.d-79)	30(n.d-45)	n.d	n.d
BaP	6(n.d - 27)	n.d	0.7(n.d-1.7)	97(n.d-170)	41(n.d-56)	22(n.d-43)	n.d
Total	**273(90-975)**	**982(30-6670)**	**45(8-216)**	**2959(451-5866)**	**2994(520-6725)**	**2404(985-5132)**	**2765(578-5097)**

n.a: not analyzed**; n.d:** not detected**; Ace:** acenaphtene**; Acy:** acenaphylene. **G:** Geispolsheim; **E:** Erstein**; STG:** Strasbourg**; CR:** Cronenbourg.

Table 4. Total PCBs concentration range (ng L^{-1}) in fog samples compared with other sites.

Site	**PCBs**	**Reference**
Zürich (Switzerland)	(7000-22000)	[44]
Northwestern Mountains (NW Spain)	(n.d-319)	[13]
Geispolsheim (France)[a]	(137-12058)	This study
Erstein (France)[b]	(434-5787)	This study
Strasbourg (France)[c]	(5383-15515)	This study
Cronenbourg (France)[d]	(934-4979)	This study

n.d: not detected.

Author Contributions: Conceptualization, D.K., M.M., Y.J., and O.D..; methodology and experimentation: D.K.; validation, D.K., M.M., Y.J., and O.D.; data curation, D.K.; writing—original draft preparation, D.K.; writing—review and editing, D.K., M.M., Y.J., and O.D.; supervision, M.M., Y.J., and O.D.; project administration, M.M. All authors have read and agreed to the published version of the manuscript.

Funding: This research received no external funding.

Data Availability Statement: Data are available upon request.

Conflicts of Interest: The authors declare no conflict of interest.

References

1. Roach, W. T. Back to Basics: Fog: Part 1 — Definitions and Basic Physics. *Weather* **1994**, *49* (12), 411–415. https://doi.org/10.1002/j.1477-8696.1994.tb05962.x.
2. Pérez-Díaz, J.; Ivanov, O.; Peshev, Z.; Álvarez-Valenzuela, M.; Valiente-Blanco, I.; Evgenieva, T.; Dreischuh, T.; Gueorguiev, O.; Todorov, P.; Vaseashta, A. Fogs: Physical Basis, Characteristic Properties, and Impacts on the Environment and Human Health. *Water* **2017**, *9* (10), 807. https://doi.org/10.3390/w9100807.
3. Khoury, D.; Millet, M.; Jabali, Y.; Delhomme, O. Fog Water: A General Review of Its Physical and Chemical Aspects. *Environments* **2023**, *10* (12), 224. https://doi.org/10.3390/environments10120224.
4. Ervens, B.; Wang, Y.; Eagar, J.; Leaitch, W. R.; Macdonald, A. M.; Valsaraj, K. T.; Herckes, P. Dissolved Organic Carbon (DOC) and Select Aldehydes in Cloud and Fog Water: The Role of the Aqueous Phase in Impacting Trace Gas Budgets. *Atmospheric Chem. Phys.* **2013**, *13* (10), 5117–5135. https://doi.org/10.5194/acp-13-5117-2013.
5. Facchini, M. C.; Fuzzi, S.; Zappoli, S.; Andracchio, A.; Gelencsér, A.; Kiss, G.; Krivácsy, Z.; Mészáros, E.; Hansson, H.; Alsberg, T.; Zebühr, Y. Partitioning of the Organic Aerosol Component between Fog Droplets and Interstitial Air. *J. Geophys. Res. Atmospheres* **1999**, *104* (D21), 26821–26832. https://doi.org/10.1029/1999JD900349.
6. Fuzzi, S.; Facchini, M. C.; Orsi, G.; Ferri, D. Seasonal Trend of Fog Water Chemical Composition in the Po Valley. *Environ. Pollut.* **1992**, *75* (1), 75–80. https://doi.org/10.1016/0269-7491(92)90059-J.
7. Mazzoleni, L. R.; Ehrmann, B. M.; Shen, X.; Marshall, A. G.; Collett, J. L. Water-Soluble Atmospheric Organic Matter in Fog: Exact Masses and Chemical Formula Identification by Ultrahigh-Resolution Fourier Transform Ion Cyclotron Resonance Mass Spectrometry. *Environ. Sci. Technol.* **2010**, *44* (10), 3690–3697. https://doi.org/10.1021/es903409k.
8. Yin, H.; Ye, Z.; Yang, Y.; Yuan, W.; Qiu, C.; Yuan, H.; Wang, M.; Li, S.; Zou, C. Evolution of Chemical Composition of Fogwater in Winter in Chengdu, China. *J. Environ. Sci.* **2013**, *25* (9), 1824–1832. https://doi.org/10.1016/S1001-0742(12)60230-7.
9. Kim, H.; Collier, S.; Ge, X.; Xu, J.; Sun, Y.; Jiang, W.; Wang, Y.; Herckes, P.; Zhang, Q. Chemical Processing of Water-Soluble Species and Formation of Secondary Organic Aerosol in Fogs. *Atmos. Environ.* **2019**, *200*, 158–166. https://doi.org/10.1016/j.atmosenv.2018.11.062.
10. Herckes, P.; Valsaraj, K. T.; Collett, J. L. A Review of Observations of Organic Matter in Fogs and Clouds: Origin, Processing and Fate. *Atmospheric Res.* **2013**, *132–133*, 434–449. https://doi.org/10.1016/j.atmosres.2013.06.005.
11. Seinfeld, J.H.; Pandis, S.N. *Atmos. Chemistry and Physics: From Air Pollution to Climate Change*, 3rd ed.; Wiley: Hoboken, NJ, USA, 2016.
12. Khoury, D.; Millet, M.; Jabali, Y.; Delhomme, O. Analytical Procedure for the Concomitant Analysis of 242 Polar and Non-Polar Organic Compounds of Different Functional Groups in Fog Water. *Microchem. J.* **2023**, *185*, 108235. https://doi.org/10.1016/j.microc.2022.108235.
13. Fernández-González, R.; Yebra-Pimentel, I.; Martínez-Carballo, E.; Simal-Gándara, J.; Pontevedra-Pombal, X. Atmospheric Pollutants in Fog and Rain Events at the Northwestern Mountains of the Iberian Peninsula. *Sci. Total Environ.* **2014**, *497–498*, 188–199. https://doi.org/10.1016/j.scitotenv.2014.07.093.
14. T. Zacharia, J. Degradation Pathways of Persistent Organic Pollutants (POPs) in the Environment. In *Persistent Organic Pollutants*; Kudom Donyinah, S., Ed.; IntechOpen, ***2019.*** https://doi.org/10.5772/intechopen.79645.
15. Castro-Jiménez, J., Eisenreich, S. J., & Vives, I. Persistent organic pollutants (POPs) in the European atmosphere: An updated overview. *European Commission Joint Research Centre*, ***2007.***
16. Meeker, J. D. Exposure to Environmental Endocrine Disruptors and Child Development. *Arch. Pediatr. Adolesc. Med.* **2012**, *166* (10). https://doi.org/10.1001/archpediatrics.2012.241.
17. Wang, J.-Z.; Nie, Y.-F.; Luo, X.-L.; Zeng, E. Y. Occurrence and Phase Distribution of Polycyclic Aromatic Hydrocarbons in Riverine Runoff of the Pearl River Delta, China. *Mar. Pollut. Bull.* **2008**, *57* (6–12), 767–774. https://doi.org/10.1016/j.marpolbul.2008.01.007.
18. Pathiratne, K. A. S.; De Silva, O. C. P.; Hehemann, D.; Atkinson, I.; Wei, R. Occurrence and Distribution of Polycyclic Aromatic Hydrocarbons (PAHs) in Bolgoda and Beira Lakes, Sri Lanka. *Bull. Environ. Contam. Toxicol.* **2007**, *79* (2), 135–140. https://doi.org/10.1007/s00128-007-9092-z.
19. Barhoumi, B.; Beldean-Galea, M. S.; Al-Rawabdeh, A. M.; Roba, C.; Martonos, I. M.; Bălc, R.; Kahlaoui, M.; Touil, S.; Tedetti, M.; Driss, M. R.; Baciu, C. Occurrence, Distribution and Ecological Risk of Trace Metals and Organic Pollutants in Surface Sediments from a Southeastern European River (Someşu Mic River, Romania). *Sci. Total Environ.* **2019**, *660*, 660–676. https://doi.org/10.1016/j.scitotenv.2018.12.428.
20. Jianrong, C.; Yanjun, L.; Sujie, Y. The Concentrations and Sources of PAHs and PCBs in Soil from an Oil Field and Estuary in the Yellow River Delta, China. *Front. Environ. Sci.* **2022**, *10*, 1028299. https://doi.org/10.3389/fenvs.2022.1028299.

21. Vane, C. H.; Kim, A. W.; Beriro, D. J.; Cave, M. R.; Knights, K.; Moss-Hayes, V.; Nathanail, P. C. Polycyclic Aromatic Hydrocarbons (PAH) and Polychlorinated Biphenyls (PCB) in Urban Soils of Greater London, UK. *Appl. Geochem.* **2014**, *51*, 303–314. https://doi.org/10.1016/j.apgeochem.2014.09.013.
22. Motelay-Massei, A.; Ollivon, D.; Garban, B.; Teil, M. J.; Blanchard, M.; Chevreuil, M. Distribution and Spatial Trends of PAHs and PCBs in Soils in the Seine River Basin, France. *Chemosphere* **2004**, *55* (4), 555–565. https://doi.org/10.1016/j.chemosphere.2003.11.054.
23. Cetin, B.; Yurdakul, S.; Gungormus, E.; Ozturk, F.; Sofuoglu, S. C. Source Apportionment and Carcinogenic Risk Assessment of Passive Air Sampler-Derived PAHs and PCBs in a Heavily Industrialized Region. *Sci. Total Environ.* **2018**, *633*, 30–41. https://doi.org/10.1016/j.scitotenv.2018.03.145.
24. Merhaby, D.; Rabodonirina, S.; Net, S.; Ouddane, B.; Halwani, J. Overview of Sediments Pollution by PAHs and PCBs in Mediterranean Basin: Transport, Fate, Occurrence, and Distribution. *Mar. Pollut. Bull.* **2019**, *149*, 110646. https://doi.org/10.1016/j.marpolbul.2019.110646.
25. Shahpoury, P.; Lammel, G.; Holubová Šmejkalová, A.; Klánová, J.; Přibylová, P.; Váňa, M. *Polycyclic Aromatic Hydrocarbons, Polychlorinated Biphenyls, and Chlorinated Pesticides in Background Air in Central Europe – Investigating Parameters Affecting Wet Scavenging of Polycyclic Aromatic Hydrocarbons*; preprint; Aerosols/Field Measurements/Troposphere/Chemistry (chemical composition and reactions), 2014. https://doi.org/10.5194/acpd-14-26939-2014.
26. Carratalá, A.; Moreno-González, R.; León, V. M. Occurrence and Seasonal Distribution of Polycyclic Aromatic Hydrocarbons and Legacy and Current-Use Pesticides in Air from a Mediterranean Coastal Lagoon (Mar Menor, SE Spain). *Chemosphere* **2017**, *167*, 382–395. https://doi.org/10.1016/j.chemosphere.2016.09.157.
27. Li, X.; Li, P.; Yan, L.; Chen, J.; Cheng, T.; Xu, S. Characterization of Polycyclic Aromatic Hydrocarbons in Fog–Rain Events. *J. Environ. Monit.* **2011**, *13* (11), 2988. https://doi.org/10.1039/c1em10543d.
28. Li, P.; Wang, Y.; Li, Y.; Wang, Z.; Zhang, H.; Xu, P.; Wang, W. Characterization of Polycyclic Aromatic Hydrocarbons Deposition in PM2.5 and Cloud/Fog Water at Mount Taishan (China). *Atmos. Environ.* **2010**, *44* (16), 1996–2003. https://doi.org/10.1016/j.atmosenv.2010.02.031.
29. Ehrenhauser, F. S.; Khadapkar, K.; Wang, Y.; Hutchings, J. W.; Delhomme, O.; Kommalapati, R. R.; Herckes, P.; Wornat, M. J.; Valsaraj, K. T. Processing of Atmospheric Polycyclic Aromatic Hydrocarbons by Fog in an Urban Environment. *J. Environ. Monit.* **2012**, *14* (10), 2566. https://doi.org/10.1039/c2em30336a.
30. ATSDR. Toxicology profile for polyaromatic hydrocarbons. *Book toxicology profile for polyaromatic hydrocarbons*. ***2005***
31. Olivella, M. À. Polycyclic Aromatic Hydrocarbons in Rainwater and Surface Waters of Lake Maggiore, a Subalpine Lake in Northern Italy. *Chemosphere* **2006**, *63* (1), 116–131. https://doi.org/10.1016/j.chemosphere.2005.07.045.
32. Erickson, M. D.; Kaley, R. G. Applications of Polychlorinated Biphenyls. *Environ. Sci. Pollut. Res.* **2011**, *18* (2), 135–151. https://doi.org/10.1007/s11356-010-0392-1.
33. Millet, M.; Sanusi, A.; Wortham, H. Chemical Composition of Fogwater in an Urban Area: Strasbourg (France). *Environ. Pollut.* **1996**, *94* (3), 345–354. https://doi.org/10.1016/S0269-7491(96)00064-4.
34. Herckes, P.; Wortham, H.; Mirabel, P.; Millet, M. Evolution of the Fogwater Composition in Strasbourg (France) from 1990 to 1999. *Atmospheric Res.* **2002**, *64* (1–4), 53–62. https://doi.org/10.1016/S0169-8095(02)00079-0.
35. Demoz, B. B.; Collett, J. L.; Daube, B. C. On the Caltech Active Strand Cloudwater Collectors. *Atmospheric Res.* **1996**, *41* (1), 47–62. https://doi.org/10.1016/0169-8095(95)00044-5.
36. Khoury, D.; Millet, M.; Weissenberger, T.; Delhomme, O.; Jabali, Y. Chemical Composition of Fogwater Collected at Four Sites in North- and Mount-Lebanon during 2021. *Atmospheric Pollution Research* **2024**, *15* (1), 101958. https://doi.org/10.1016/j.apr.2023.101958.
37. De Luca, G.; Furesi, A.; Leardi, R.; Micera, G.; Panzanelli, A.; Costantina Piu, P.; Sanna, G. Polycyclic Aromatic Hydrocarbons Assessment in the Sediments of the Porto Torres Harbor (Northern Sardinia, Italy). *Mar. Chem.* **2004**, *86* (1–2), 15–32. https://doi.org/10.1016/j.marchem.2003.11.001.
38. Larsen, R. K.; Baker, J. E. Source Apportionment of Polycyclic Aromatic Hydrocarbons in the Urban Atmosphere: A Comparison of Three Methods. *Environ. Sci. Technol.* **2003**, *37* (9), 1873–1881. https://doi.org/10.1021/es0206184.
39. Delhomme, O.; Rieb, E.; Millet, M. POLYCYCLIC AROMATIC HYDROCARBONS ANALYZED IN RAINWATER COLLECTED ON TWO SITES IN EAST OF FRANCE (STRASBOURG AND ERSTEIN). *Polycycl. Aromat. Compd.* **2008**, *28* (4–5), 472–485. https://doi.org/10.1080/10406630802377898.
40. Atmo grand est, *atmo-grandest.eu*. ***2019***
41. Yang, X.; Wang, L.; Zhang, A.; Liu, X.; Bidegain, G.; Zong, H.; Guan, C.; Song, M.; Qu, L.; Huang, W.; Yuan, X. Levels, Sources and Potential Risks of Polychlorinated Biphenyls and Organochlorine Pesticides in Sediments of Qingduizi Bay, China: Does Developing Mariculture Matter? *Front. Mar. Sci.* **2019**, *6*, 602. https://doi.org/10.3389/fmars.2019.00602.

42. Babut, M.; Miege, C.; Villeneuve, B.; Abarnou, A.; Duchemin, J.; Marchand, P.; Narbonne, J. F. Correlations between Dioxin-like and Indicators PCBs: Potential Consequences for Environmental Studies Involving Fish or Sediment. *Environ. Pollut.* **2009**, *157* (12), 3451–3456. https://doi.org/10.1016/j.envpol.2009.06.016.
43. Van Den Berg, M.; Birnbaum, L. S.; Denison, M.; De Vito, M.; Farland, W.; Feeley, M.; Fiedler, H.; Hakansson, H.; Hanberg, A.; Haws, L.; Rose, M.; Safe, S.; Schrenk, D.; Tohyama, C.; Tritscher, A.; Tuomisto, J.; Tysklind, M.; Walker, N.; Peterson, R. E. The 2005 World Health Organization Reevaluation of Human and Mammalian Toxic Equivalency Factors for Dioxins and Dioxin-Like Compounds. *Toxicol. Sci.* **2006**, *93* (2), 223–241. https://doi.org/10.1093/toxsci/kfl055.
44. Capel, P. D.; Leuenberger, C.; Giger, W. Hydrophobic Organic Chemicals in Urban Fog. *Atmospheric Environ. Part Gen. Top.* **1991**, *25* (7), 1335–1346. https://doi.org/10.1016/0960-1686(91)90244-2.